Published in final edited form as:
*Dent Mater*. 2008 May ; 24(5): 700–707.

# Analysis of Subcritical Crack Growth in Dental Ceramics Using Fracture Mechanics and Fractography

**Burak Taskonak**[1], **Jason A. Griggs**[1], **John J. Mecholsky Jr.**[2], and **Jia-Hau Yan**[2]

1 *Department of Biomaterials Science, Baylor College of Dentistry, Texas A&M University, System Health Science Center, University of Florida*

2 *Department of Materials Science and Engineering, College of Engineering, University of Florida*

## Abstract

**Objectives—**The aim of this study was to test the hypothesis that the flexural strengths and critical flaw sizes of dental ceramic specimens will be affected by the testing environment and stressing rate even though their fracture toughness values will remain the same.

**Methods—**Ceramic specimens were prepared from an aluminous porcelain (Vitadur Alpha; VITA Zahnfabrik, Bad Säckingen, Germany) and an alumina-zirconia-glass composite (In-Ceram® Zirconia; VITA Zahnfabrik). Three hundred uniaxial flexure specimens (150 of each material) were fabricated to dimensions of 25 mm × 4 mm × 1.2 mm according to the ISO 6872 standard. Each group of 30 specimens was fractured in water using one of four different target stressing rates ranging on a logarithmic scale from 0.1 to 100 MPa/s for Vitadur Alpha and from 0.01 to 10 MPa/s for In-Ceram® Zirconia. The fifth group was tested in inert environment (oil) with a target stressing rate of 100 MPa/s for Vitadur Alpha and 1000 MPa/s for In-Ceram® Zirconia. The effects of stressing rate and environment on flexural strength, critical flaw size, and fracture toughness were analyzed statistically by Kruskal-Wallis one-way ANOVA on ranks followed by post-hoc comparisons using Dunn's test ($\alpha$=0.05). In addition, 20 Vitadur Alpha specimens were fabricated with controlled flaws to simplify fractography. Half of these specimens were fracture tested in water and half in oil at a target stressing rate of 100 MPa/s, and the results were compared using Mann-Whitney rank sum tests ($\alpha$=0.05). A logarithmic regression model was used to determine the fatigue parameters for each material.

**Results—**For each ceramic composition, specimens tested in oil had significantly higher strength ($P \leq 0.05$) and smaller critical flaw size (significant for Vitadur Alpha, $P \leq 0.05$) than those tested in water but did not have significantly different fracture toughness ($P > 0.05$). Specimens tested at faster stressing rates had significantly higher strength ($P \leq 0.05$) but did not have significantly different fracture toughness ($P > 0.05$). Regarding critical flaw size, stressing rate had a significant effect for In-Ceram® Zirconia specimens ($P \leq 0.05$) but not for Vitadur Alpha specimens ($P > 0.05$). Fatigue parameters, $n$ and ln $B$, were 38.4 and −12.7 for Vitadur Alpha and were 13.1 and 10.4 for In-Ceram® Zirconia.

**Significance—**Moisture assisted subcritical crack growth had a more deleterious effect on In-Ceram® Zirconia core ceramic than on Vitadur Alpha porcelain. Fracture surface analysis identified

Corresponding author: Jason A. Griggs, PhD, (Now at) Department of Biomedical Materials Science, The University of Mississippi Medical Center, 2500 North State Street, Jackson, MS 39216-4505, Phone: + 1-601-984-6173, Fax: + 1-601-984-6087, e-mail: JGriggs@sod.umsmed.edu.

fracture surface features that can potentially mislead investigators into misidentifying the critical flaw.

**Keywords**

Dental ceramic; Fracture surface analysis; Subcritical crack growth; Stressing rate; Testing environment

## 1. Introduction

The improved toughness and strength of dental ceramics has increased their clinical use in multi-unit fixed partial dentures [1–6]. However, toughness and initial strength of dental ceramics are not the only factors that determine long-term survival. Subcritical crack growth (SCG) significantly decreases survival time of dental ceramics [7]. SCG is crack propagation at stress intensity factor ($K_I$) levels lower than the critical stress intensity factor, or fracture toughness ($K_C$) [8–10]. Long-term or repetitive low-level loading may cause pre-existing subcritical flaws to slowly grow until failure occurs at a level of loading that was insufficient to cause failure of the virgin prosthesis.

For *in vitro* testing, stressing rate dependence of strength is a characteristic sign of SCG [11]. Every specimen will fracture when it reaches the critical stress intensity factor, but quickly stressed specimens will reach that point sooner. This allows less time for stress-corrosion to increase the crack size [11]. If fracture toughness is constant, then a smaller critical flaw translates into higher failure stress.

The amount of SCG is affected by several other factors in addition to stressing rate [12]. The rate of SCG is a power law function of stress intensity factor [9]. The shapes of the flaws within the material affect the stress intensity factor such that sharp flaws and flaws with high depth-to-width ratios correspond to greater stress intensity factor at the same stress level and hence faster SCG than blunt flaws and flaws with low depth-to-width ratios [13]. Additionally, the presence of moisture usually has a deleterious effect [14]. In dental applications fractures occur in an aqueous environment. However, Griffith and Irwin fracture mechanics equations assume that fracture takes place in a chemically inert environment [15,16]. Environment can have a strong effect on crack growth, with aqueous environments leading to more SCG and hence lower strength than inert environments [7]. However, some ceramic compositions react with water to blunt sharp flaws on the ceramic surface, resulting in increased strength in aqueous environments [10,17,18]. Thus, survivability of dental ceramics depends on the loading time as well as the initial flaw size distribution and flaw shapes.

Since dental ceramics perform over long periods of time in the presence of moisture, it seems likely that the degree of susceptibility to SCG will be a major factor in determining their survivability. SCG of various dental ceramics has been investigated using cyclic, static, and dynamic loading methods [7,19–33]. Analyzing the SCG for both veneer and core components of the same all-ceramic system would enable lifetime prediction using finite element models. For this reason, In-Ceram® Zirconia and Vitadur Alpha were selected for this study.

The primary goal of this study was to analyze the effects, if any, of the stressing rate and testing environment on the flexural strength, critical flaw size, and fracture toughness of a zirconia-based dental core ceramic and glass veneer. Two hypotheses were proposed:

1. The critical flaw sizes of core and veneer specimens will be controlled by the presence of water and changing stressing rates in the testing environment due to SCG.

2. The flexural strengths of specimens will decrease with the decreasing stressing rate in a water testing environment, however, their fracture toughness will remain the same.

## 2. Materials and methods

This study was performed on two different dental ceramics that are widely used in fabricating all-ceramic dental fixed prostheses. A glass-based veneering dental ceramic (Vitadur Alpha; VITA Zahnfabrik, Bad Säckingen, Germany) was chosen to exemplify materials that are used as veneering materials in ceramic fixed partial dentures. An alumina-zirconia-glass composite (In-Ceram® Zirconia; VITA Zahnfabrik) was chosen to exemplify materials that are used as core materials due to their relatively higher failure strength and fracture toughness. The composition of In-Ceram® Zirconia as purported by the manufacturer is (mol%) 62 $Al_2O_3$, 20 $SiO_2$, 11–15, 12 $La_2O_3$, 4.5 $SiO_2$, 0.8 CaO, 0.7 other oxides [34]. The composition of Vitadur Alpha as purported by the manufacturer is (mol%) 66–70 $SiO_2$, 11–14 $Al_2O_3$, 4–5 $B_2O_3$, 3–4 $Na_2O$, 7–9 $K_2O$, 1–2 CaO, and < 0.1 $TiO_2$ [personal communication]. Three hundred uniaxial flexure specimens (150 Vitadur Alpha, 150 In-Ceram® Zirconia) were fabricated to dimensions of 25 mm × 4 mm × 1.2 mm according to the ISO 6872 standard [35]. All specimens were fired and treated according to the manufacturer's recommendations. Any specimen that according to ISO 6872 had excessive porosity on the surface to be placed in tension was eliminated.

Vitadur Alpha specimens were fabricated by mixing 0.5 g of ceramic powder (VITA Zahnfabrik) and 0.18 g of modeling liquid (VITA Zahnfabrik) to form a slurry. The slurry was poured into custom fabricated steel molds with dimensions of 25.50 mm × 4.75 mm × 2.00 mm. Then, the slurry was condensed in the molds using a mechanical vibrator (No. 1A; Buffalo Dental, Syosset, NY, USA) followed by manual vibration to allow any trapped air to escape from the mold. A firing cycle was performed using a dental porcelain furnace (Centurion Q200; Ney, Yucaipa, CA, USA) according to the manufacturer's instructions as follows: The specimens were dried at 600°C for 6 min, heated to 960°C at a rate of 60°C/min under full vacuum, held at 960°C for 1 min, and subsequently cooled for one minute before removing the specimens from the furnace. After completing the firing cycle, bench-cooling to room temperature was performed for all specimens. An additional firing cycle was performed as follows: The specimens were dried at 600°C for 6 min, heated to 950°C at a rate of 58°C/min under full vacuum, held at 950°C for 1 min, and subsequently cooled for one minute before removing the specimens from the furnace. All specimens were ground to the final desired dimensions of 25 mm × 4 mm × 1.2 mm, and the tensile surfaces were polished using SiC abrasive papers with sequentially finer grit size (U.S. Industrial grit # 180, 240, 320, 400 and 600) (8" Plain Back Silicon Carbide Discs; Allied High Tech Products, Rancho Dominguez, CA, USA). The polishing sequence was the same for all the specimens, and the last polishing direction was performed along the long axis of the specimen. All the specimens were auto-glazed as follows: Each specimen was dried at 600°C for 4 min, heated to 920°C at a rate of 107°C/min, and held for 1 min at 920°C; this firing cycle was run under atmospheric pressure. Subsequently, all specimens were bench-cooled to room temperature.

A very thin (0.05 mm) adhesive tape (Scotch® Magic™ Tape; 3M, St. Paul, MN, USA) was placed on the compressive surface to secure the fractured segments of the specimen during the fracture test. The specimens were assigned randomly into five groups of 30 specimens each. One group of specimens was tested under an inert environment. The other specimens were tested while immersed in deionized water at 37°C. The inert strength specimens were heated at 140°C for 14 hours to remove any moisture from the specimens, and then they were placed in 140°C SAE 85W-140 oil (Super Tech; Wal-Mart Stores, Bentonville, AR, USA), and allowed to cool to 37°C in a desiccator to prevent atmospheric moisture from contacting the specimens. This should have prevented moisture from assisting crack growth during fracture.

In-Ceram® Zirconia specimens were fabricated to the dimensions of 25 mm × 4 mm × 1.2 mm. This was accomplished by cutting ceramic blocks (Zirconia ZB-80; VITA Zahnfabrik) into the desired shape and dimensions using a low-speed saw with a diamond cutting blade (Isomet; Buehler, Lake Bluff, IL, USA). The ceramic block was mounted on the cutting arm, which was adjusted by an attached micrometer to set the desired cut thickness. Zirconia ZB-80 blocks are porous; to fill all open porosity a glass infiltration procedure was performed. This was performed by applying a coating of glass powder-water slurry (In-Ceram® Zirconia Glass Powder; VITA Zahnfabrik) to the ceramic specimens using a dental ceramic brush. The specimens were placed in a programmable vacuum porcelain furnace (Multimat® Touch & Press; Dentsply, York, PA, USA) to perform the glass infiltration firing cycle according to the manufacturer's recommendations as follows: All specimens were dried at 600°C for 1 min, heated to 1140°C at a rate of 20°C/min, and held at 1140°C for 40 min under full vacuum. After glass infiltration, the excess glass was removed using heatless coarse-grained SiC wheels (Mizzy Heatless® Wheels; Keystone, Cherry Hill, NJ, USA). Following this step, the In-Ceram® Zirconia specimens were treated exactly as the Vitadur Alpha specimens, and all the firing steps that were performed on the Vitadur Alpha specimens were also performed on the In-Ceram® Zirconia specimens, since in the clinical situation a veneer of Vitadur Alpha will be built on top of an In-Ceram® Zirconia core, and accordingly, the core material will encounter all the firing cycles that the veneer encounters.

In addition, two extra groups (n=10) of specimens were prepared from Vitadur Alpha, and one group was tested in oil whereas the other group was tested in water both at 37°C using a stressing rate of 100 MPa/s. These specimens were indented on their tensile surfaces to produce controlled flaws. The purpose of these specimens was to confirm the data obtained from fractographic analysis of specimens where inherent flaws were present. Indentation cracks were induced within the tensile surface of all specimens using a Vickers indenter with a 0.5° angle slope at a load of 4.9 N to produce controlled flaws. Critical flaw sizes can be measured with certainty in indented specimens using fractography [36].

Four-point flexure testing was performed using a servohydraulic mechanical testing machine (Minibionix 858; MTS Systems Corporation, Eden Prairie, MN, USA) with a custom semi-articulating four-point flexure fixture having an outer span of 20 mm and an inner span of 10 mm. The target stressing rates were attained using the mechanical testing machine in load-controlled mode. Equation 3 was used to determine the load rates necessary to reach the target stressing rates with an assumed width and thickness.

$$\dot{P} = \frac{4}{3}\frac{\dot{\sigma}}{L}wt^2 \tag{1}$$

where $\dot{P}$ is the load rate, $\dot{\sigma}$ is the target stressing rate, $L$ is the outer (support) span of the test fixture, $w$ is the specimen width, and $t$ is the specimen thickness. Each group of Vitadur Alpha specimens was fractured using one of four different target stressing rates ranging on a logarithmic scale from 0.1 to 100 MPa/s. The fifth group was tested in inert environment (oil) with a target stressing rate of 100 MPa/s. Different target stressing rates, which ranged from 0.01 to 10 MPa/s, were used for the In-Ceram® Zirconia specimens, and a target stressing rate of 1000 MPa/s was used for the inert strength group. The width and thickness of each specimen were measured adjacent to the fracture surface to determine the flexural strength, $\sigma_f$, of each specimen according to the following equation:

$$\sigma_f = \frac{3PL}{4wt^2} \tag{2}$$

where $P$ is the maximum load recorded during testing. The actual stressing rate, $\dot{\sigma}_{Actual}$, for each specimen was determined individually using the following equation:

$$\dot{\sigma}_{Actual} = \frac{\sigma_f}{t_f} \tag{3}$$

where $t_f$ is the failure time determined from the four-point flexure test for each specimen.

Ritter derived the flexural strength equation for materials tested under constant stressing rate as [11]:

$$\sigma_f^{n+1} = B(n+1)S_i^{n-2}\,\dot{\sigma} \tag{4}$$

where $\dot{\sigma}$ is the stressing rate, and $S_i$ is the inert (moisture free) flexural strength. By performing regression of ln $\sigma_f$ vs. ln $\dot{\sigma}$, a linear model of best fit can be constructed and used to estimate the SCG parameters, $n$ and $B$.

To determine the fracture origins of the specimens, the fracture surfaces of the tested specimens were coated with gold-palladium using a sputter-coating machine (Technics Inc., Alexandria, VA, USA). Each specimen was studied with a stereomicroscope (Bauch & Lomb Inc., Rochester, NY, USA) at 160X magnification. Crack initiating flaws were measured to determine the fracture toughness of each specimen. Scanning electron microscope (JSM-6400, Jeol, Tokyo, Japan) examination was performed on selected specimens and SEM images were recorded from representative fracture surfaces.

Fracture toughness, $K_C$, was calculated using fractographic analysis and the fracture mechanics equation:

$$K_C = Y\sigma_f a^{\frac{1}{2}} \tag{5}$$

where $Y$ is a geometric factor that was calculated using Newman-Raju equations based on the shape of the critical flaw [37], $\sigma_f$ is the calculated flexural strength, and $a$ is the depth of the critical flaw. For purposes of comparing critical flaw sizes, the size of an equivalent semi-circular flaw, $c$, was calculated using the depth, $a$, and half width, $b$, of the semi-elliptical flaw on the fracture surface [38,39].

$$c = (ab)^{\frac{1}{2}} \tag{6}$$

The data were not normally distributed (Kolmogorov-Smirnov $P \leq 0.05$), and the number of valid specimens varied between groups, so Kruskal-Wallis one-way analysis of variance on ranks followed by Dunn's test ($\alpha$=0.05) were used to determine whether the differences between group medians for flexural strength, critical flaw size, and fracture toughness of specimens were statistically significant.

Twenty-four specimens with inherent internal flaws or edge cracks were excluded from the study to obtain a statistical analysis within specimens that had semi-elliptical surface fracture origins only.

## 3. Results

Descriptive statistics for flexural strength, critical flaw size, and fracture toughness of each group are summarized in Tables 1 and 2 for Vitadur Alpha and In-Ceram® Zirconia, respectively. Median flexural strength values increased with increasing stressing rate and were higher for oil environment than for water environment. The differences in median strength values of the groups tested in oil and water were statistically significant ($P \leq 0.05$) from each other within each material. A significant difference was found between the median flexural strengths of Vitadur Alpha groups tested in water at different stressing rates ($P \leq 0.05$). There

were also significant differences between median flexural strengths of In-Ceram® Zirconia groups tested at or below 0.1 MPa/s versus above 0.1 MPa/s (P>0.05).

There were no statistical differences between the median fracture toughness values of Vitadur Alpha groups tested in oil and tested at the same stressing rate in water (P>0.05) nor between those tested at different stressing rates in water (P>0.05). In-Ceram® Zirconia groups also represented the same data trend where no statistical difference in median fracture toughness values was seen based on chemical environment (P>0.05) or stressing rate (P>0.05).

Median critical flaw sizes diminished with increasing stressing rate and were smaller for oil environment than for water environment. For In-Ceram® Zirconia, there was no significant difference between the median critical flaw sizes of the group tested in water at 10 MPa/s and the group tested in oil at 1000 MPa/s (P>0.05). However, there was a difference in median critical flaw sizes between groups tested at or below 0.1 MPa/s versus above 0.1 MPa/s in water (P≤0.05). Although, Vitadur Alpha specimens showed a similar trend, the differences based on chemical environment were significant (P≤0.05) whereas the differences based on testing rate were not significant (P>0.05).

Fractographic analysis of specimens revealed that failure originated either from voids (internal flaws) (Figure 1a), edge cracks (Figure 1b), or surface flaws, which were semi-elliptical in shape (Figure 1c). Surface porosity was the most common initial flaw for both materials. Specimens with inherent internal flaws or edge cracks exhibited lower failure stresses.

Specimens with indentation controlled flaws confirmed the data from specimens with inherent flaws (Table 1). The controlled flaw Vitadur Alpha specimens tested in water had significantly lower median flexural strength (P<0.001) and significantly larger median critical flaw size (P<0.001) than those tested in oil, but there was no significant difference in median fracture toughness values (P=0.386).

Regression of ln flexural strength versus ln stressing rate provided fatigue exponents, $n$, of 38.4 and 13.1 for Vitadur Alpha and In-Ceram® Zirconia, respectively, and fatigue intercepts, ln $B$, of 12.7 and −10.4, respectively (Figures 2 and 3).

## 4. Discussion

Zirconia-based ceramics are expected to be good structural materials because of high strength and wear resistance. In most cases zirconia is stabilized by yttria to control volume change due to phase transformation mechanism. On the other hand, strength degradation occurs in zirconia ceramics when they are used in water environment due to the chemical reaction of yttria with water leading to the depletion of yttria [40–42]. In addition, when zirconia is used in multiphase ceramic composites like alumina-zirconia-glass dental ceramics, it is likely that the glass phase will be the dominant factor controlling the SCG [7].

A clear indication of the effect of SCG in Vitadur Alpha and In-Ceram® Zirconia was the difference in flexural strengths of specimens tested in water and those tested in oil. In addition, fractography confirmed that the same difference can be observed between the flaw sizes of the specimens tested in water and those tested in oil (Tables 1 and 2).

In silicate glasses, at low crack velocities, crack propagation is controlled primarily by chemical reactions at the crack tip between water and the Si-O bond [43]; in this region, the amount of time for crack extension to occur by this mechanism depends on the stressing rate [11,44]. Figures 2 and 3 show dynamic fatigue data for the In-Ceram® Zirconia and Vitadur Alpha in water at 37°C. A decrease of flexural strength with decreasing stressing rate is clear in these plots. Based on the data in Figures 2 and 3 and Equation 5, the SCG parameter $n$ was calculated

to be 38.4 for the Vitadur Alpha. In comparison, the *n*-value was determined to be 13.1 for the In-Ceram® Zirconia, which indicates a greater susceptibility to SCG for In-Ceram® Zirconia. This might be due to the fact that grain-boundaries between glass and crystalline phases are more vulnerable than glass matrix phases to chemical attack by water molecules under stress corrosion conditions. As a result, cracks propagate preferentially along grain boundaries [45, 46]. Although In-Ceram® Zirconia has less glass phase than does Vitadur Alpha, In-Ceram® Zirconia should have more glass phase boundary area, since it is a 3-3 composite material. Furthermore, the phase boundaries are continuous throughout the microstructure [47].

Fractographic analysis of the specimens confirmed the SCG for specimens tested in a water environment. Michalske described the fracture surface patterns due to regions I, II and III crack growth of soda-lime silica glass tested in water [10]. In this study, besides the statistically significant difference between the critical flaw sizes of specimens tested in water and those tested in oil, fracture patterns of specimens tested in water indicated slow crack growth before catastrophic fracture. In the specimens tested in water, specifically in the low stress intensity factor ($K_I$) region, water corrodes the crack tip, thereby altering the crack geometry. Wake hackle markings, known as “fracture tails” were observed at pores on the fracture surfaces (Figure 4a). These markings were helpful in determining the crack direction and critical flaw location. Primary Wallner lines were observed on the fracture surfaces of some specimens (Figure 4a). These markings are produced by the intersection of a propagating crack with sonic pulses, which are typically initiated by the interaction of the crack with discontinuities on the tensile surface. They were helpful in determining the fracture origin in those specimens. The Wallner lines were more prominent on the specimens fractured in water. In many cases two oppositely oriented Wallner lines intersected at a point between the critical flaw and neutral axis, giving the mistaken appearance of a larger critical flaw (Figure 4a). Careful attention should be paid during fracture surface analysis because misidentification of a Wallner line pair as the critical flaw would lead to erroneous fracture toughness values calculated using Equation 4. This study contained groups with controlled indentation cracks to confirm the data obtained from specimens with inherent flaws. The authors initially made an error in measuring critical flaw sizes, which was corrected after predicting the anticipated critical flaw sizes using Equation 4. This required prior knowledge of the fracture toughness, which was determined using the specimens with controlled indentation cracks (Figure 4b). It is clear that fractographic analysis is essential to fracture toughness evaluation in humid environments [10].

## 5. Conclusions

The hypothesis that the critical flaw sizes of core and veneer specimens will be controlled by the presence of the water and changing stressing rates in the testing environment due to SCG was verified. The hypothesis that the flexural strength of ceramic bars will decrease with slower stressing rates in a water testing environment was also verified; however, their fracture toughness will remain the same.

The flexural strength, critical flaw sizes, and fracture patterns of In-Ceram® Zirconia and Vitadur Alpha dental ceramics loaded in flexure were governed by the testing environment and stressing rate, but the fracture toughness is a material property, which is independent of the experimental factors in this study.

#### Acknowledgements

This investigation was supported by research grant DE013358 from the National Institute of Dental and Craniofacial Research, National Institutes of Health, Bethesda, MD.

We appreciate the advice of Mr. George Quinn in the fracture surface analysis of specimens for this paper.

The ceramic materials used in this study were donated by Vident, Brea, CA.

## References


1. Esquivel-Upshaw JF, Anusavice KJ, Young H, Jones J, Gibbs C. Clinical performance of a lithia disilicate-based core ceramic for three-unit posterior FPDs. Int J Prosthodont 2004;17:469–75. [PubMed: 15382785]
2. Qualtrough AJE, Piddock V. Ceramics update. J Dent 1997;25:91–5. [PubMed: 9105138]
3. Taskonak B, Mecholsky JJ Jr, Anusavice KJ. Residual stresses in bilayer dental ceramics. Biomaterials 2005;26:3235–41. [PubMed: 15603818]
4. Suárez MJ, Salido MP, Martínez F. Three-year clinical evaluation of In-Ceram® Zirconia posterior FPDs. Int J Prosthodont 2004;17:35–8. [PubMed: 15008230]
5. Kelly J. Ceramics in restorative and prosthetic dentistry. Annu Rev Mater Sci 1997;27:443–68.
6. Scurria MS, Bader JD, Shugars DA. Meta-analysis of fixed partial denture survival: Prostheses and abutments. J Prosthet Dent 1998;79:459–64. [PubMed: 9576323]
7. Zhu QS, de With G, Dortmans LJ, Feenstra F. Subcritical crack growth behavior of Al2O3- glass dental composites. J Biomed Mater Res B 2003;65B:233–8.
8. Lawn, BR. Fracture of Brittle Solids. 2. Cambridge: Cambridge University Press; 1993. p. 106-12.
9. Weiderhorn, SM. Subcritical crack growth in ceramics. In: Bradt, RC.; Hasselman, DPH.; Lange, FF., editors. Fracture Mechanics of Ceramics. New York, NY: Plenum Press; 1974. p. 613-46.
10. Michalske, TA. Fractography of slow fracture in glass. In: Mecholsky, JJ., Jr; Powell, SR., Jr, editors. Fractography of Ceramic and Metal Failures. Washington, DC: American Society for Testing and Materials; 1984. p. 121-36.
11. Ritter, JE. Engineering design and fatigue failure of brittle materials. In: Lange, FF., editor. Fracture Mechanics of Ceramics. New York, NY: Plenum Press; 1978. p. 613-46.
12. Glasstone, S.; Laidler, KJ.; Eyring, H. The Theory of Rate Processes. New York, NY: McGraw-Hill; 1941. p. 65-68.
13. Mecholsky JJ Jr, Freiman SW, Rice RW. Effect of grinding on flaw geometry and fracture of glass. J Am Ceram Soc 1977;60:114–7.
14. Michalske TA, Smith WL, Bunker BC. Fatigue mechanisms in high-strength silica-glass fibers. J Am Ceram Soc 1991;74:1993–6.
15. Griffith AA. The phenomena of rupture and flow in solids. Phil Trans Roy Soc Lond 1920;A221:163.
16. Irwin, GR. Handbuch der Physik. Berlin: Springer-Verlag; 1958. Fracture; p. 551
17. Tomozawa M. Fracture of glasses. Annu Rev Mater Sci 1996;26:43–74.
18. Griggs JA, Kishen A, Le KN. Mechanism of strength increase for a hydrothermal porcelain. Dent Mater 2003;19:625–31. [PubMed: 12901987]
19. Fairhurst CW, Lockwood PE, Ringle RD, Twiggs SW. Dynamic fatigue of feldspathic porcelain. Dent Mater 1993;9:269–73. [PubMed: 7988760]
20. Twiggs SW, Fairhurst CW, Lockwood PE, Ringle RD. Cyclic fatigue of a model feldspathic porcelain. Dent Mater 1995;11:273–6. [PubMed: 8621051]
21. Anusavice KJ, Lee RB. Effect of firing temperature and water exposure on crack propagation in unglazed porcelain. J Dent Res 1989;68:1075–81. [PubMed: 2808866]
22. Azer SS, Drummond JL, Campbell SD, El Moneim Zaki A. Influence of core buildup material on the fatigue strength of an all-ceramic crown. J Prosthet Dent 2001;86:624–31. [PubMed: 11753315]
23. Chen HY, Hickel R, Setcos JC, Kunzelmann KH. Effects of surface finish and fatigue testing on the fracture strength of CAD-CAM and pressed-ceramic crowns. J Prosthet Dent 1999;82:468–75. [PubMed: 10512968]
24. Drummond JL, King TJ, Bapna MS, Koperski RD. Mechanical property evaluation of pressable restorative ceramics. Dent Mater 2000;16:226–33. [PubMed: 10762684]
25. Jung YG, Peterson IM, Kim DK, Lawn BR. Lifetime-limiting strength degradation from contact fatigue in dental ceramics. J Dent Res 2000;79:722–31. [PubMed: 10728973]
26. Myers ML, Ergle JW, Fairhurst CW, Ringle RD. Fatigue failure parameters of IPS-Empress porcelain. Int J Prosthodont 1994;7:549–53. [PubMed: 7748450]
27. Myers ML, Ergle JW, Fairhurst CW, Ringle RD. Fatigue characteristics of a high-strength porcelain. Int J Prosthodont 1994;7:253–7. [PubMed: 7916891]

28. Ohyama T, Yoshinari M, Oda Y. Effects of cyclic loading on the strength of all-ceramic materials. Int J Prosthodont 1999;12:28–37. [PubMed: 10196825]
29. Peterson IM, Wuttiphan S, Lawn BR, Chyung K. Role of microstructure on contact damage and strength degradation of micaceous glass-ceramics. Dent Mater 1998;14:80–9. [PubMed: 9972155]
30. Sobrinho LC, Cattell MJ, Glover RH, Knowles JC. Investigation of the dry and wet fatigue properties of three all-ceramic crown systems. Int J Prosthodont 1998;11:255–62. [PubMed: 9728120]
31. White SN. Mechanical fatigue of a feldspathic dental porcelain. Dent Mater 1993;9:260–4. [PubMed: 7988758]
32. White SN, Zhao XY, Zhaokun Y, Li ZC. Cyclic mechanical fatigue of a feldspathic dental porcelain. Int J Prosthodont 1995;8:413–20. [PubMed: 8595099]
33. White SN, Li Y, Yu Z, Kipnis V. Relationship between static chemical and cyclic mechanical fatigue in a feldspathic porcelain. Dent Mater 1997;13:103–10. [PubMed: 9467312]
34. Borges GA, Sophr AM, De Goes MF, Sobrinho LC, Chan DCN. Effect of etching and airborne particle abrasion on the microstructure of different dental ceramics. J Prosthet Dent 2003;89:479–88. [PubMed: 12806326]
35. ISO. 6872 Dental Ceramic. Geneva, Switzerland: International Organization for Standardization; 1995.
36. ASTM. 1421-01b Standard Test Method for Determination of Fracture Toughness of Advanced Ceramics at Ambient Temperature. West Conshohocken, PA: ASTM International; 2001.
37. Newman JC, Raju IS. An empirical stress-intensity factor equation for the surface crack. Eng Fract Mech 1981;15:185–92.
38. Mecholsky, JJ, Jr. Quantitative fractographic analysis of fracture origins in glass. In: Bradt, RC.; Tressler, RE., editors. Fractography of Glass. New York, NY: Plenum Press; 1994. p. 39-73.
39. Mecholsky JJ Jr. Fractography: Determining the sites of fracture initiation. Dent Mater 1995;11:113–6. [PubMed: 8621031]
40. Yoshimura M, Noma T, Kawabata K, Somiya S. Role of H2O on the degradation process of Y-TZP. J Mater Sci Lett 1987;6:465–7.
41. Chevalier J, Olagnon C, Fantozzi G. Subcritical crack propagation in 3Y-TZP ceramics: Static and cyclic fatigue. J Am Ceram Soc 1999;82:3129–38.
42. Piconi C, Maccauro G. Zirconia as a ceramic biomaterial. Biomaterials 1999;20:1–25. [PubMed: 9916767]
43. Michalske T, Freiman S. A molecular interpretation of stress corrosion in silica. Nature 1982;295:511–2.
44. McElhaney KW, Ma Q. Investigation of moisture-assisted fracture in SiO2 films using a channel cracking technique. Acta Materialia 2004;52:3621–9.
45. Mecholsky JJ Jr. Intergranular slow crack-growth in MgF2. J Am Ceram Soc 1981;64:563–6.
46. Kirchner HP, Gruver RM. Fractographic criteria for subcritical crack-growth boundaries in 96-percent Al2O3. J Am Ceram Soc 1980;63:169–74.
47. Giordano R, Pelletier L, Campbell S, Pober R. Flexural strength of an infused ceramic, glass- ceramic, and feldspathic porcelain. J Prosthet Dent 1995;73:411–8. [PubMed: 7658388]

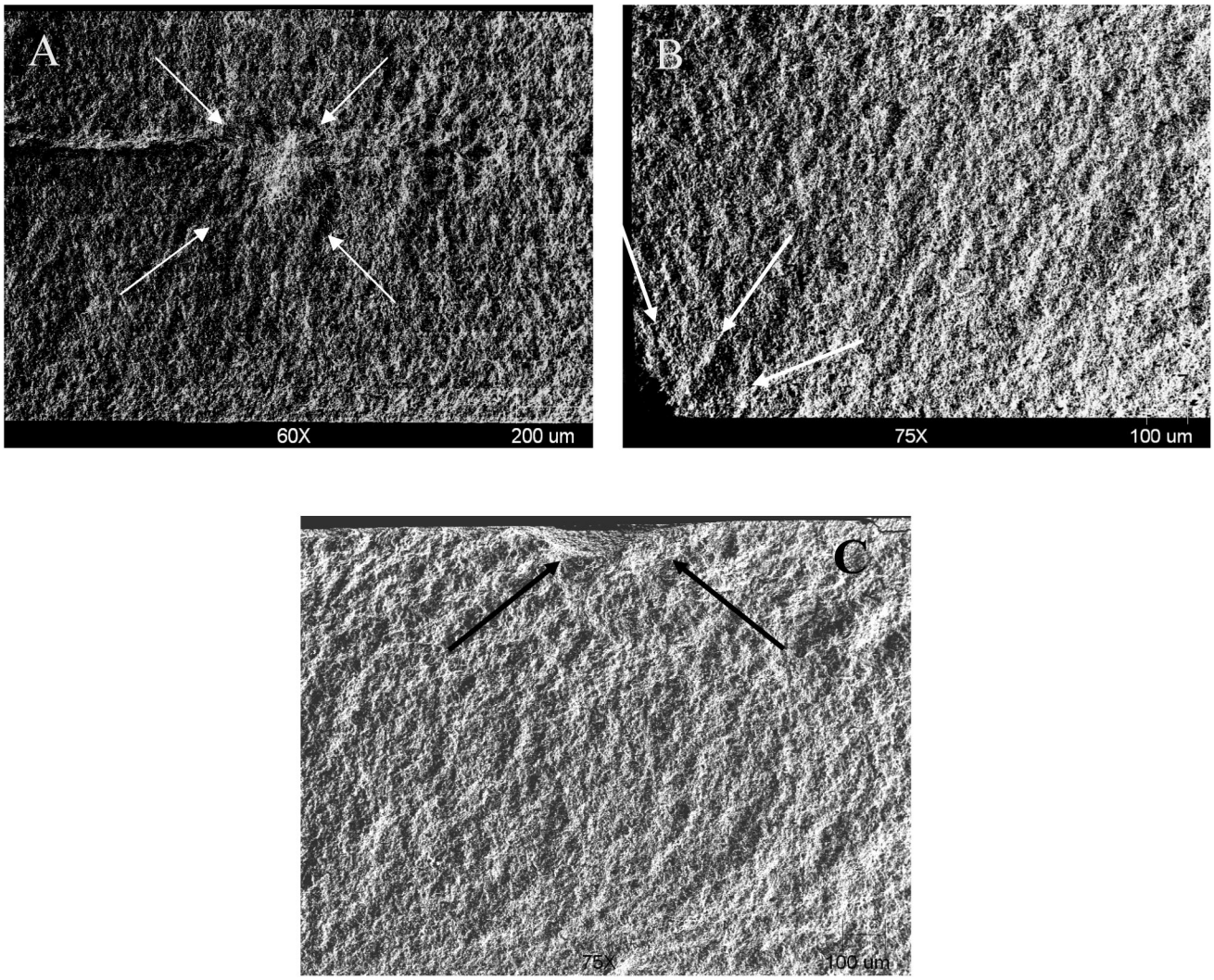


**Figure 1.**
Fracture surfaces (SEM view). (A) The fracture origin (arrows) of an In-Ceram® Zirconia specimen failed from an internal flaw. (B) The fracture origin (arrows) of an In-Ceram® Zirconia specimen failed from edge crack. (C) The fracture origin (arrows) of an In-Ceram® Zirconia specimen failed from a semi-elliptical surface flaw.

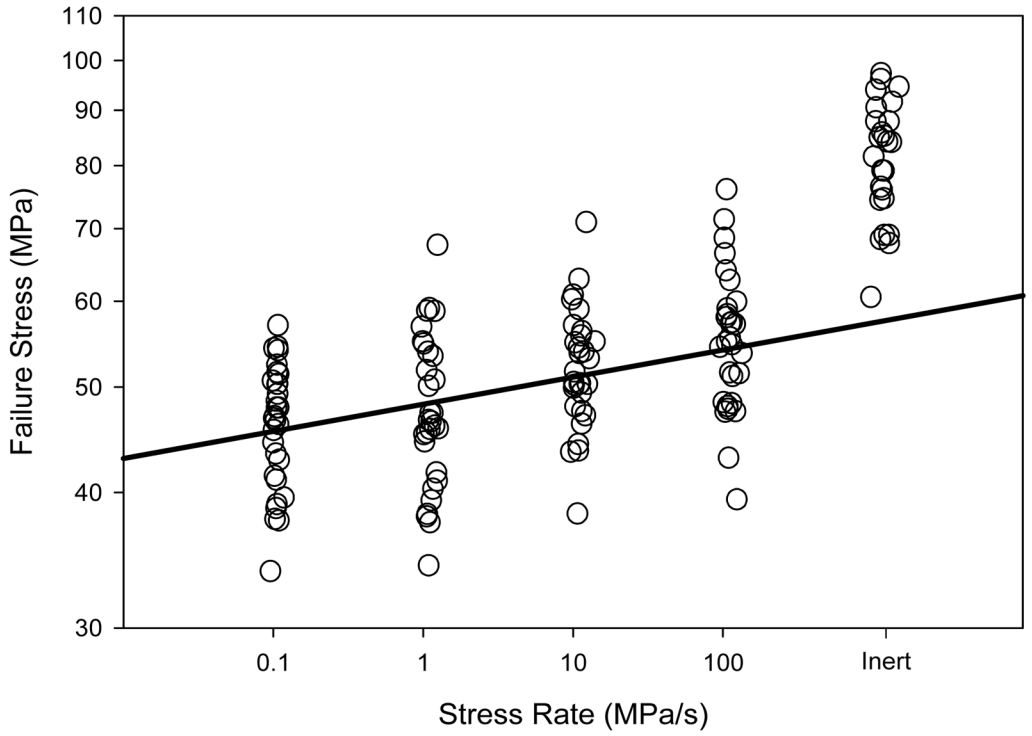


**Figure 2.**
Flexural strength data as a function of stressing rate for the Vitadur Alpha flexure specimens tested in water. Solid line is ln-ln regression model through median points.

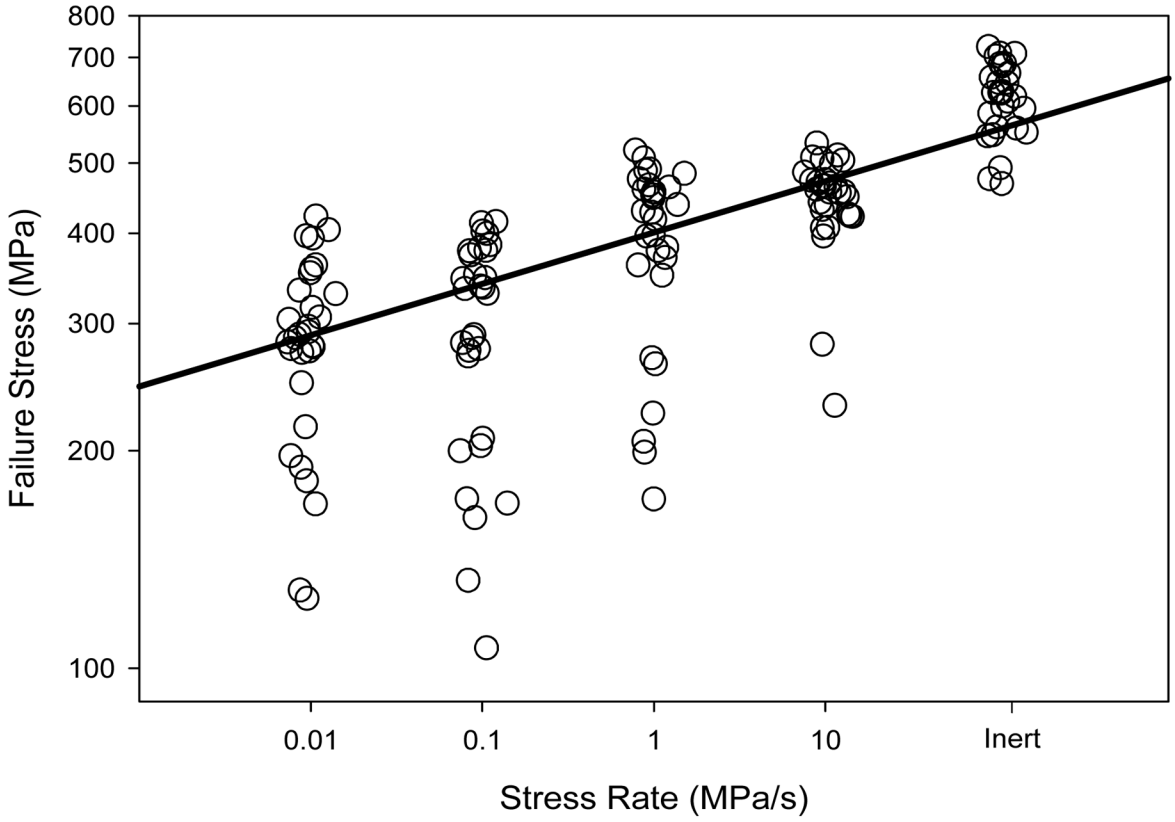


**Figure 3.**
Flexural strength data as a function of stressing rate for the In-Ceram® Zirconia flexure specimens tested in water. Solid line is ln-ln regression model through median points.

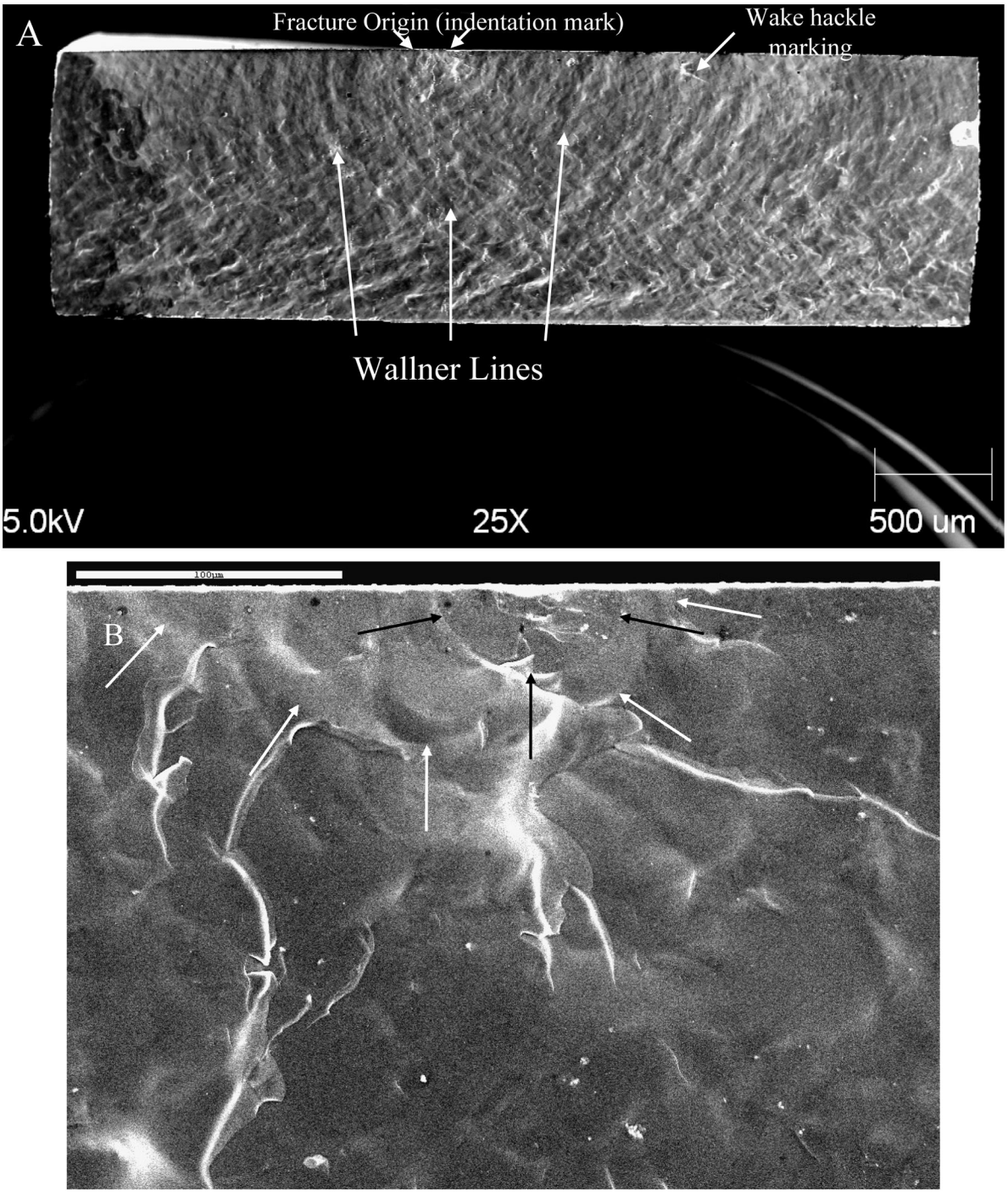


**Figure 4.**
Fracture surface (SEM) of an indented Vitadur Alpha specimen tested in water. (A) Various surface features that were formed during crack growth are labeled. (B) Higher magnification of the same specimen showing the indentation induced semi-elliptical crack (black arrows) and critical flaw (white arrows).

**Table 1**

Median (interquartile range) of flexural strength (σ), critical flaw size (c), and fracture toughness ($K_c$) values of Vitadur Alpha monolithic ceramic bars.

| Testing environment | Stressing rate | σ (MPa) | c (μm) | $K_c$ (Mpa·$m^{1/2}$) |
|---|---|---|---|---|
| **Water** | **0.1 MPa/s** | 46.9(41.4–50.6) | 109(97–139) | 0.58(0.51–0.65) |
| **Water** | **1 MPa/s** | 46.5(41.7–53.8) | 115(84–128) | 0.60(0.54–0.70) |
| **Water** | **10 MPa/s** | 51.0(47.9–55.7) | 92(65–114) | 0.58(0.54–0.63) |
| **Water** | **100 MPa/s** | 55.3(48.4–59.0) | 109(94–121) | 0.67(0.60–0.76) |
| **Oil** | **100 MPa/s** | 85.0(75.9–94.5) | 39(33–54) | 0.72(0.69–0.79) |
| **Oil (Indented)** | **100 MPa/s** | 78.4(75.6–97.4) | 34(26–35) | 0.60(0.56–0.63) |
| **Water (Indented)** | **100 MPa/s** | 46.2(44.4–49.6) | 110(104–123) | 0.62(0.59–0.63) |

**Table 2**

Median (interquartile range) of flexural strength (σ), critical flaw size (c), and fracture toughness ($K_c$) values of In-Ceram® Zirconia monolithic ceramic bars.

| Testing environment | Stressing rate | σ(MPa) | c (μm) | $K_c$ (Mpa·$m^{1/2}$) |
|---|---|---|---|---|
| **Water** | **0.01 MPa/s** | 305(283–355) | 146(116–163) | 4.5(4.3–4.9) |
| **Water** | **0.1 MPa/s** | 346(287–383) | 128(111–140) | 4.6(3.8–5.0) |
| **Water** | **1 MPa/s** | 449(396–470) | 103(80–114) | 5.4(4.7–5.6) |
| **Water** | **10 MPa/s** | 461(433–479) | 101(87–111) | 5.5(5.2–5.7) |
| **Oil** | **1000 MPa/s** | 624(559–668) | 65(50–71) | 5.6(5.2–6.2) |